Journal of Sustainable Metallurgy
https://doi.org/10.1007/s40831-024-00811-8

RESEARCH ARTICLE

# Thermodynamic Investigations for Combustion-Assisted Synthesis of Lithium Orthosilicate Powders

**Kağan Benzeşik**[1] · **Onuralp Yücel**[1]

Received: 18 December 2023 / Accepted: 7 March 2024


## Abstract

The study investigates the combustion-assisted synthesis of lithium orthosilicate ($Li_4SiO_4$) powders for potential $CO_2$ capture applications. Technical-grade lithium carbonate and metallic silicon powders were used as starting materials. Synthesis conditions were explored across temperatures ranging from 500 to 900 °C and different holding durations. Thermodynamic modeling using FactSage 8.2 software suggested that $Li_4SiO_4$ production is feasible at temperatures of 700 °C and higher with metallic silicon as the silicon source, which was confirmed experimentally. Characterization of the synthesized powders involved X-ray diffraction, specific surface area determination, particle size distribution analysis, scanning electron microscopy, and $CO_2$ uptake tests. Despite having the lowest $Li_4SiO_4$ content as 83.7%, the sample synthesized at 700 °C with 45 min of holding time showed the best $CO_2$ uptake performance as 12.80 wt% while having the lowest crystallite size value (126.58 nm), the highest specific surface area value (4.975 $m^2/g$) and the lowest average particle size value (10.85 µm) which are highly effective on the $CO_2$ uptake performance of such solid sorbents. The study concludes that while challenges remain in achieving optimal $CO_2$ capture performance, it lays a foundation for utilizing lithium orthosilicate in carbon capture applications.

### Graphical Abstract

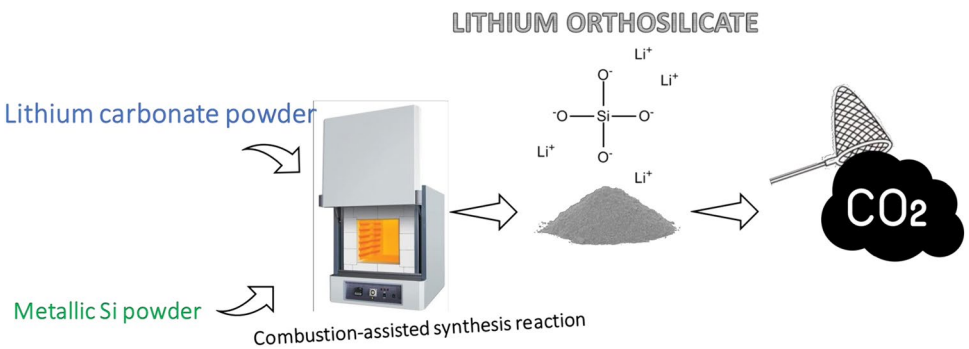


**Keywords** Combustion synthesis · Lithium orthosilicate · Ceramic sorbent · $CO_2$ capture

## Introduction

One of the most significant common challenges facing humanity in recent years is environmental degradation caused by the uncontrolled release of carbon dioxide ($CO_2$) into the atmosphere. The rapid growth of industry and cities in developing nations has resulted in a substantial increase in carbon emissions. This surge in the global concentration

The contributing editor for this article was João António Labrincha Batista.

✉ Kağan Benzeşik
benzesik@itu.edu.tr

[1] Faculty of Chemical-Metallurgical Engineering, Metallurgical and Materials Engineering Department, Istanbul Technical University, Istanbul, Turkey

Published online: 25 March 2024

of greenhouse gases, notably $CO_2$, due to human activities is causing global warming and consequential climate change [1]. Climate change indeed has far-reaching global consequences, including reduced agricultural productivity due to factors like decreased rainfall, unpredictable seasons, and rising temperatures [2]. As a result of climate change, numerous regions across the globe are experiencing unsuitability for commercial agriculture due to drought conditions. The persistent shifts in temperature and precipitation patterns are exacerbating issues related to water scarcity and soil degradation [3]. If the present rate of human-induced pollution and the uncontrolled emission of greenhouse gases into the atmosphere persist, experts predict that the ongoing challenges of global warming, ocean acidification, desertification, and unpredictable weather patterns will deteriorate further.

Power generation plants that rely on fossil fuels are recognized as one of the primary sources of greenhouse gas emissions, particularly $CO_2$, which is a major contributor to global warming [4, 5]. Incorporating these emissions into the equation, data from the National Oceanic and Atmospheric Administration (NOAA) Global Monitoring Laboratory (GML), a division of the Earth System Research Laboratories (ESRL), reveals that atmospheric $CO_2$ levels have surged from approximately 340 parts per million (ppm) during the 1980s to 419 ppm as of the start of 2023 [6].

The carbon capture and storage (CCS) method has gained recognition as a crucial means to mitigate atmospheric $CO_2$ levels [7]. CCS involves a three-step process: (i) capturing $CO_2$ from flue gases, (ii) transporting the captured $CO_2$ for storage in geological formations, and (iii) permanently removing $CO_2$ from the atmosphere over the long term [8].

Carbon capture and storage (CCS) systems typically employ three primary pathways for $CO_2$ capture: pre-combustion, oxy-fuel combustion, and post-combustion $CO_2$ capture. In the pre-combustion approach, $CO_2$ capture occurs before fossil fuel combustion. This involves a gasification process that generates no pollutant gases and ensures efficient capture performance. Oxy-fuel combustion involves the use of pure oxygen instead of ambient air during the combustion process. As a result, the flue gas produced at the end of this process contains a high concentration of $CO_2$, which creates a favorable environment for the separation and removal of $CO_2$ from the system [9, 10]. True to its name, the post-combustion process involves capturing $CO_2$ from the flue gas after the combustion has taken place. This approach is often viewed as advantageous due to its adaptability to existing power plants, making it a feasible option for retrofitting carbon capture technology [9].

Currently, amine scrubbing, often employing an aqueous monoethanolamine (MEA) solution, is recognized as one of the most advanced technologies for $CO_2$ capture. However, it's important to note that $CO_2$ removal through MEA scrubbing is considered energy-inefficient, as the regeneration process typically consumes approximately 20–30% of the output of a typical power plant [11]. Additionally, commonly used amine-based solvents are susceptible to degradation and oxidation, rendering them corrosive and necessitating potentially hazardous material handling procedures [12].To address these drawbacks, the use of solid sorbents is emerging as an alternative. This approach has the potential to reduce the energy required for solvent transportation and regeneration by more than 30% [13]. Among the various solid sorbents, lithium orthosilicate ($Li_4SiO_4$) stands out as a promising option. This is primarily due to its excellent $CO_2$ capture properties, which include higher capacity, faster kinetics, durability in cyclic use, and a relatively lower regeneration temperature (below 800 °C) when compared to other high-temperature solid sorbents [14–19].

Traditionally, lithium orthosilicate ($Li_4SiO_4$) is produced using a solid-state synthesis method. This method involves mixing powdered lithium carbonate ($Li_2CO_3$) as the source of lithium and powdered silicon dioxide ($SiO_2$) as the source of silicon. The mixture is then subjected to high-temperature calcination which leads a relatively high amounts of energy consumption [20–22]. For example, solid-state synthesis may involve temperatures ranging from 800 to 1100 °C and take around 7 to 8 h. These high-temperature processes can lead to issues like lithium evaporation and the formation of a liquid phase, which can inhibit the formation of the desired $Li_4SiO_4$ phase [23–25].

Combustion synthesis has emerged as an alternative to traditional production methods for creating advanced materials and powders, including ceramics (both structural and functional), composites, alloys, intermetallic compounds, and nano-materials. This approach is gaining attention due to its simplicity and favorable techno-economic conditions. The fundamental concept behind combustion synthesis relies on self-propagating reactions with high exothermicity. Consequently, combustion synthesis is recognized as an energy-efficient production method [26–28]. Given these advantages, combustion synthesis has also found application as an alternative method for producing high-temperature solid sorbents [14, 29].

The primary objective of this study is to produce lithium orthosilicate ($Li_4SiO_4$) material, which shows promise as a solid sorbent for $CO_2$ capture. Instead of relying on traditional methods with high energy consumption, the study explores alternative methods for $Li_4SiO_4$ production. Additionally, the research aims to identify the properties that influence the $CO_2$ capture performance of $Li_4SiO_4$-based powders. In the initial phase of the experimental investigations, the production of $Li_4SiO_4$ powders, as a solid sorbent for $CO_2$ capture, was undertaken using combustion synthesis method, diverging from the conventional

solid-state synthesis approach. The study focused on optimizing the production steps of $Li_4SiO_4$ powders through solid-state combustion synthesis (SHS). Notably, this study marks the first attempt to produce $Li_4SiO_4$ powders through SHS, contributing valuable insights to the existing literature on the topic. In the second part of the experimental studies, the $CO_2$ capture performances of $Li_4SiO_4$ powders produced by combustion synthesis methods were evaluated. $CO_2$ capture tests of the obtained powders were completed in a thermogravimetric analyzer.

## Experimental

### Materials

Technical grade lithium carbonate powder ($Li_2CO_3$, ≥ 99.0) as lithium source and metallic silicon powder (Si, Alfa Aesar, -325 mesh) as silicon source were selected for the synthesis studies. All these raw materials were used directly without any pretreatment and further purification.

### Synthesis of Lithium Orthosilicate Powders

Prior to the synthesis studies, a phase equilibrium diagram between $Li_2O$ and $SiO_2$ was generated using "phase diagram" module of FactSage 8.2 software and presented in Fig. 1. As it is seen from the diagram, pure $Li_4SiO_4$ phase can be achieved while keeping the $SiO_2$ addition as 0.333 mol.

Lithium orthosilicate powders were synthesized by a combustion-assisted synthesis reaction given below which is in line with the phase diagram given above. After stoichiometric amounts of $Li_2CO_3$ and metallic Si powders were weighed based on 10 g of $Li_2CO_3$ according to Eq. (1), the initial powders were mixed by a turbula mixer for 15 min in order to obtain homogeneous mixtures.

$$2Li_2CO_3 + Si + O_2 \rightarrow Li_4SiO_4 + 2CO_2 \quad (1)$$

Then, the powders were put into alumina boats which have 100 × 30x12 mm dimensions (Fig. 2.). Boats were put in a muffle furnace in order to conduct the synthesis reaction. Heating started from room temperature up to temperatures 500—900 °C for optimizing the reaction

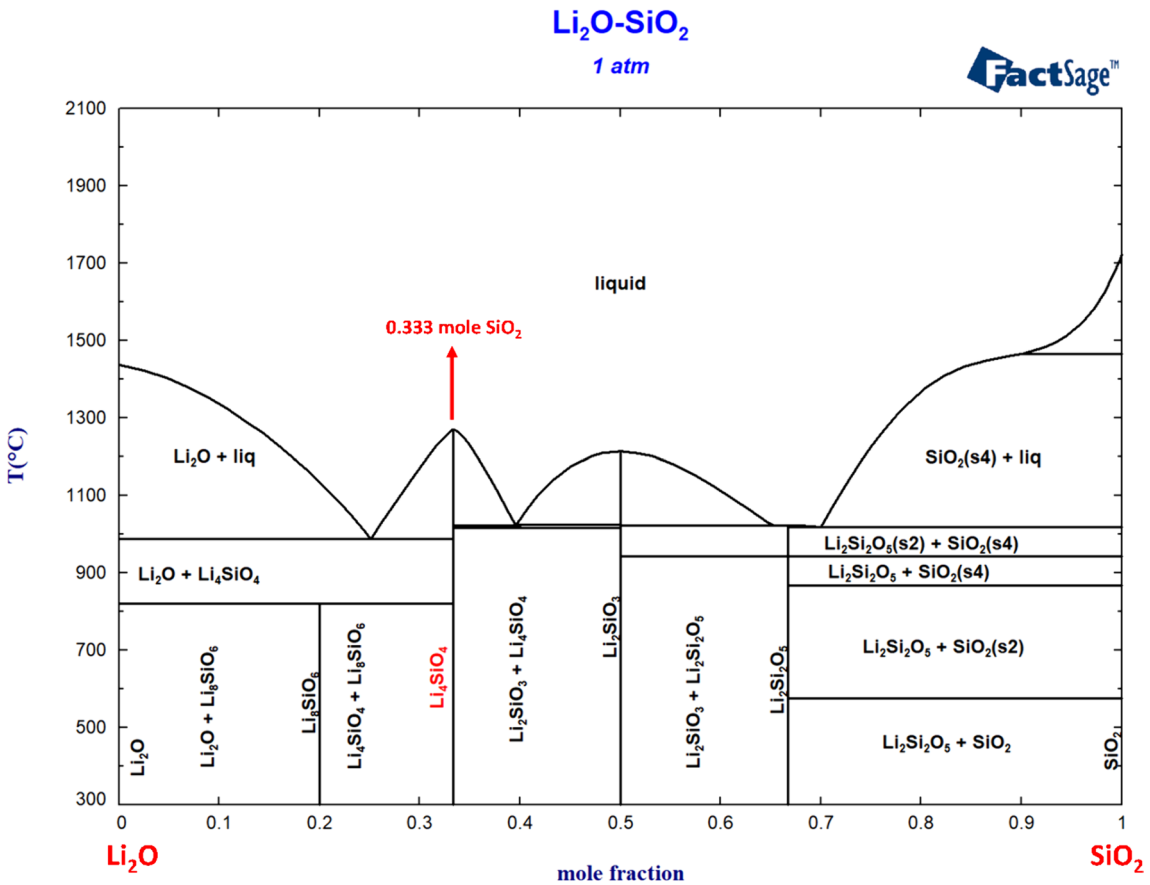


**Fig. 1** Phase equilibrium diagram of $Li_2O$-$SiO_2$ system

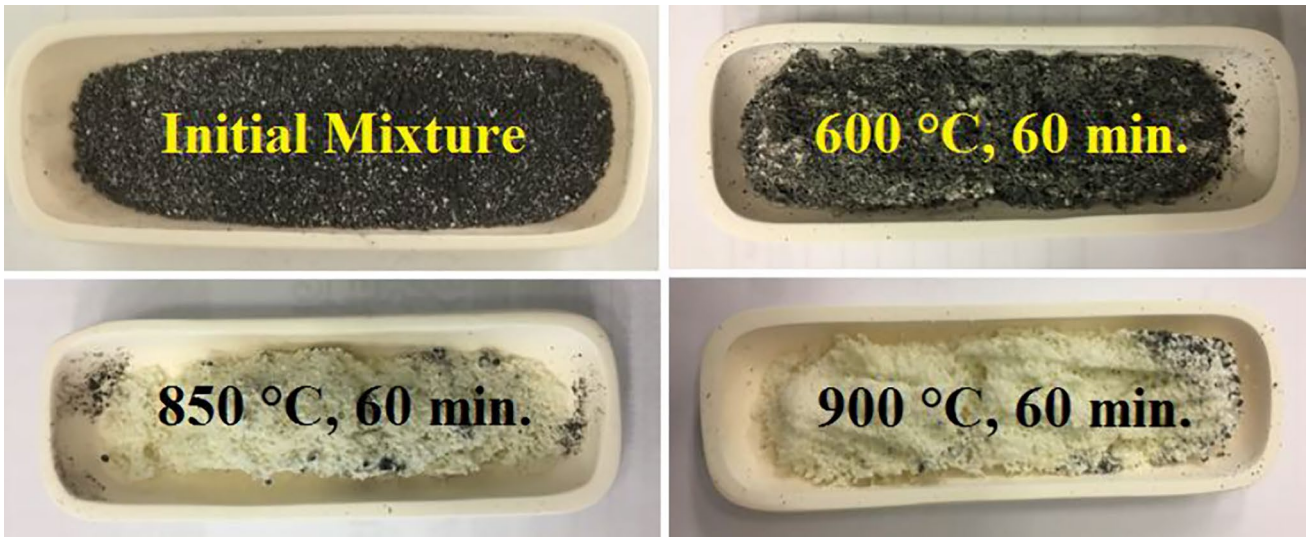


**Fig. 2** Color change of the products depending on the synthesis temperature

temperature with the holding duration of 60 min. After synthesis duration was complete, products were left to cool down to room temperature inside the furnace. Then, the products were grinded manually using an agate mortar and subjected to further characterizations.

Once the temperature was optimized, 45 and 75 min of holding durations were also studied for the temperatures which have resulted in higher weight loss, in other words, higher conversion rates. All the experiment parameters are given in Table 1.

**Table 1** Experimental parameters

| Exp. No | Temp, °C | Duration, min | Heating rate, °C/min |
|---|---|---|---|
| 1 | 500 | 60 | 5 |
| 2 | 550 | | |
| 3 | 600 | | |
| 4 | 650 | | |
| 5 | 700 | | |
| 6 | 750 | | |
| 7 | 675 | | |
| 8 | 800 | | |
| 9 | 850 | | |
| 10 | 900 | | |
| 11 | 700 | 75 | 5 |
| 12 | 750 | | |
| 13 | 800 | | |
| 14 | 850 | | |
| 15 | 900 | | |
| 16 | 700 | 45 | 5 |
| 17 | 750 | | |
| 18 | 800 | | |
| 19 | 850 | | |
| 20 | 900 | | |

## Characterization Techniques

Thermodynamic modeling of synthesis studies was carried out with FactSage 8.2 thermochemical simulation software. Adiabatic temperature, specific heat and possible product outputs were simulated [30].

X-ray diffraction technique using a Bruker D8 Advanced Series equipment (operated at 35 kV and 40 mA) with CuKα ($\lambda = 1.5406$ A) radiation at 2θ range of 10–90° with a step size of 0.02° and a rate of 2°/ min was applied for the phase analysis of the synthesized powders. Conversion rates of the products were determined according to phase quantification results performed by Rietveld refinement using Malvern Panalytical XPert HighScore Plus software. Crystallite size calculations were completed by BrukerTM-AXS TOPAS 4.2 software using Lorentzian approach. Specific surface area determination was carried out by $N_2$ physisorption at 77 °K by Micromeritics ASAP2020 with performing the Brunauer, Emmett, and Teller (BET) method according to the ISO 9277 Standard. The particle size distribution of the products was determined by Beckman Coulter LS 13320 equipment according to the ISO 13320 Standard using laser diffraction technique. The morphologies of the powders were examined by scanning electron microscopy (ThermoFisher, Axia ChemiSEM).

### *$CO_2$ Sorption Tests*

The $CO_2$ sorption performance of synthesized powders was evaluated using a thermogravimetric analyzer (Setaram Setsys Evolution). Tests were carried out under a flow rate of 65 ml/min with a gas atmosphere of 92 vol% $CO_2$ (balance $N_2$). Samples were first pre-treated for 30 min at 100 °C under $N_2$, then they were heated with a heating rate of 20 °C/min up to 600 °C (sorption temperature) under a stream of pure $N_2$. Once the sorption temperature was reached and stabilized for 10 min, the gas was switched to 92 vol% $CO_2$ (balance $N_2$) and sorption lasted for 120 min [22].

## Results and Discussion

### Thermodynamic Investigations

Prior to the experimental studies, the production conditions and reaction thermodynamics of $Li_4SiO_4$ powders by combustion assisted solid state reaction synthesis were modeled with FactSage 8.2 software. For comparison, the production conditions of $Li_4SiO_4$ powders by solid-state synthesis were also modeled. The enthalpy and Gibbs free energy changes of the reactions were simulated using the "reaction" module of the software without applying any initial conditions. Thus, the thermodynamic data between the reaction inputs and products were obtained dependent on the changing reaction temperature. While simulating the synthesis products, "equilibrium" module was operated. The "FactPS" database was chosen for both "reaction" and "equilibrium" module operation.

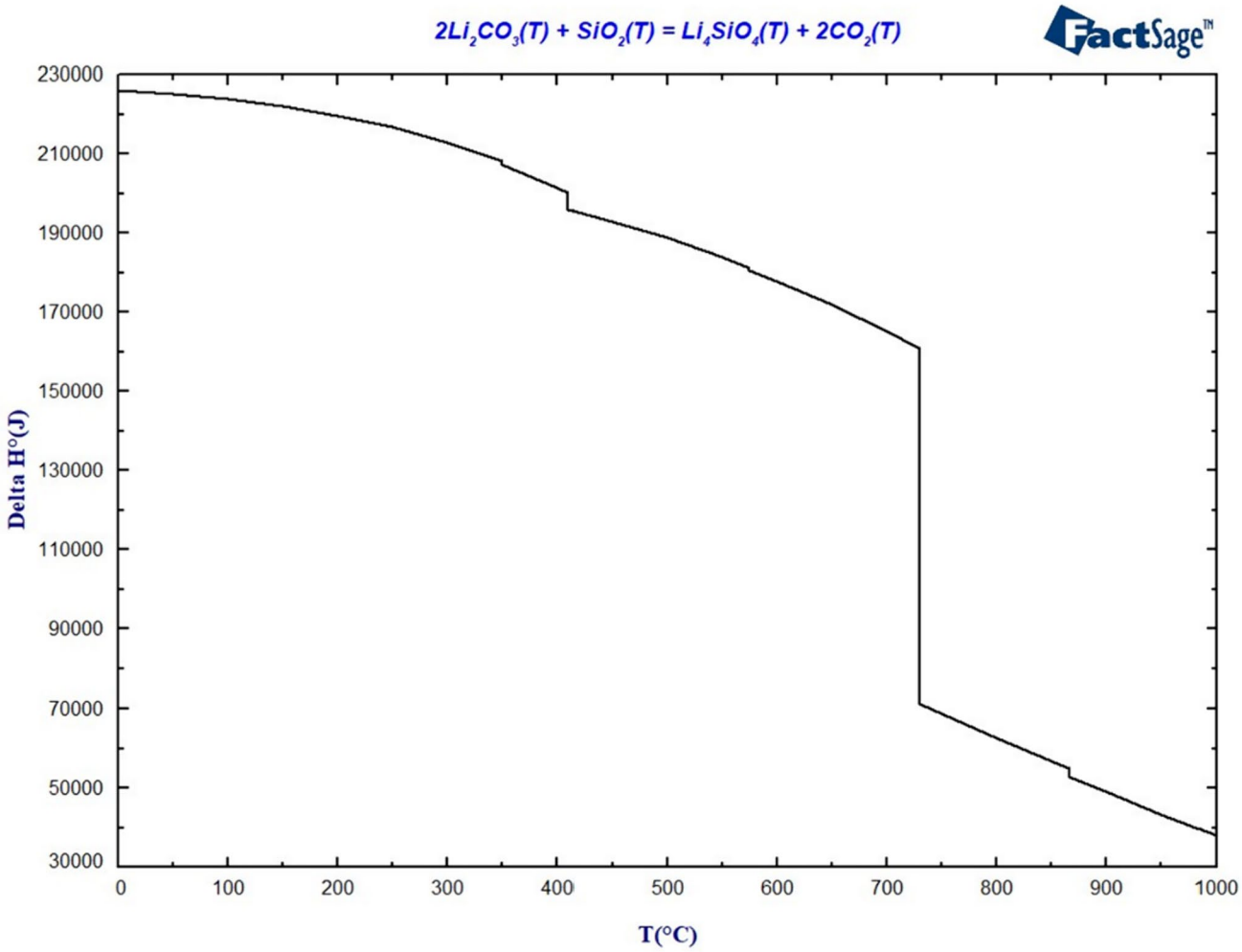


**Fig. 3** The enthalpy change of the solid-state synthesis reaction

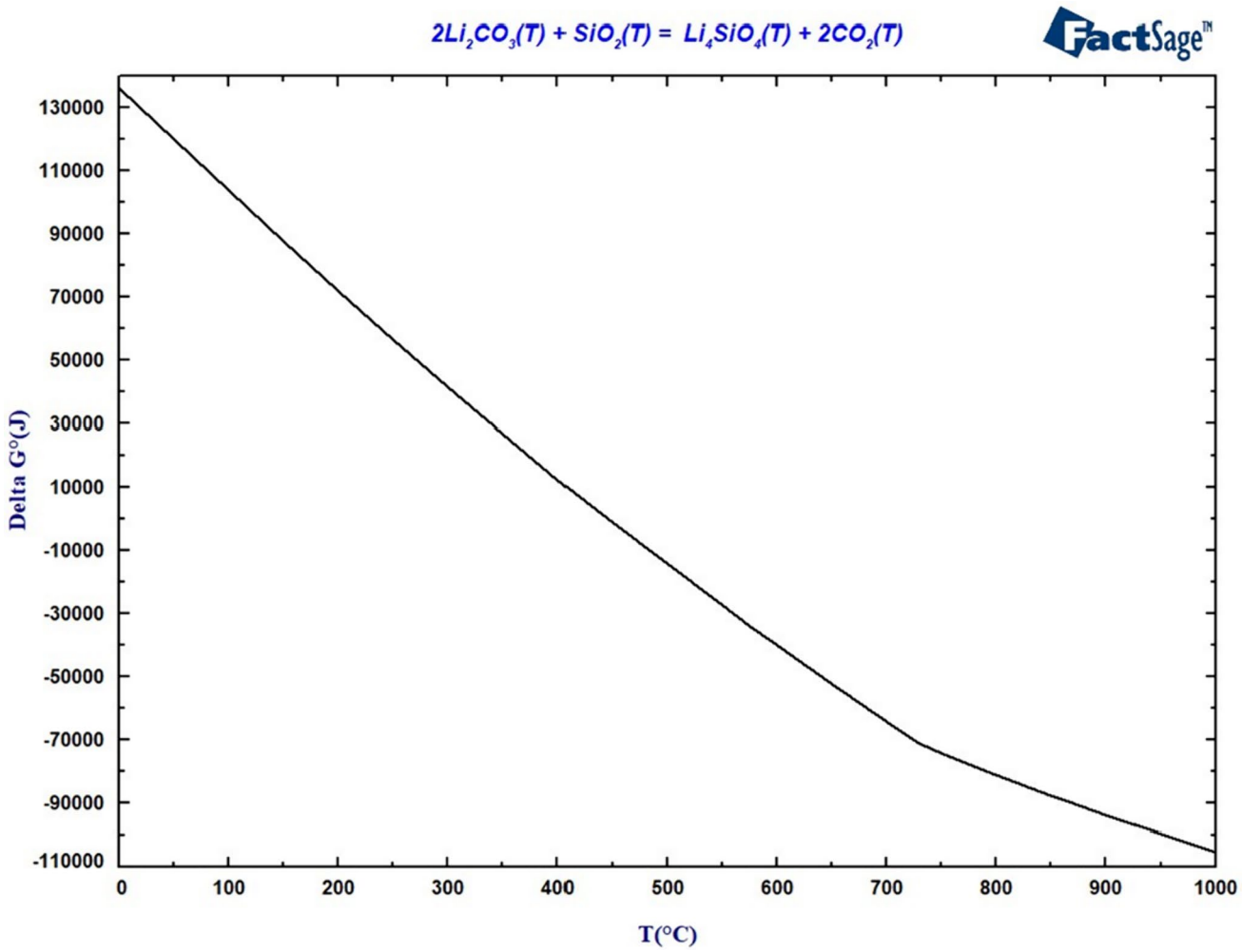


**Fig. 4** The Gibbs free energy change of the solid-state synthesis reaction

The enthalpy and Gibbs free energy changes of the solid-state synthesis reaction are shown in Fig. 3 and Fig. 4 respectively. When the enthalpy change graph is examined, it is seen that the enthalpy change value decreased from approximately 160.000 J to 70.000 J at 700 °C as a result of endothermic reaction during solid state synthesis. The reason for this was determined as the transformation of $Li_4SiO_4$. Similarly, the breaks at 350 and 400 °C are due to polymorphic transformations of $Li_2CO_3$. These transformations are clearly visible in the modeling of $Li_4SiO_4$ production by solid state synthesis shown in Fig. 7.

When the Gibbs free energy change graph was examined, it was determined that the Gibbs free energy change values decreased with increasing synthesis temperature, but solid-state synthesis is possible at temperatures higher than 450 °C.

The enthalpy change plot of the combustion-assisted synthesis reaction (Fig. 5) shows that this reaction is exothermic. When the starting mixture was heated to 700 °C, a large increase in the amount of energy released during the reaction was observed. The enthalpy change value at this temperature increased from approximately -740.000 J to -830.000 J. This change indicates that combustion and $Li_4SiO_4$ transformation takes place at 700 °C. This transformation can be clearly seen in the modeling of $Li_4SiO_4$ production by combustion-assisted synthesis reaction given in Fig. 8.

The Gibbs free energy change graph (Fig. 6.) of the combustion-assisted synthesis reaction reveals that production of $Li_4SiO_4$ is thermodynamically possible at all temperatures.

Similarly, the $T_{ad}$ values of the solid-state synthesis reaction, combustion-assisted synthesis reaction and the combustion reaction of silicon with oxygen at 800 °C were modeled. $T_{ad} = 598$ °C for solid state synthesis, $T_{ad} = 2049$ °C for combustion-assisted synthesis reaction and $T_{ad} = 2874$ °C for the $Si + O_2 = SiO_2$ reaction. In other words, when the starting mixture is heated to 800 °C, the solid-state synthesis reaction utilizes this heat energy supplied to the

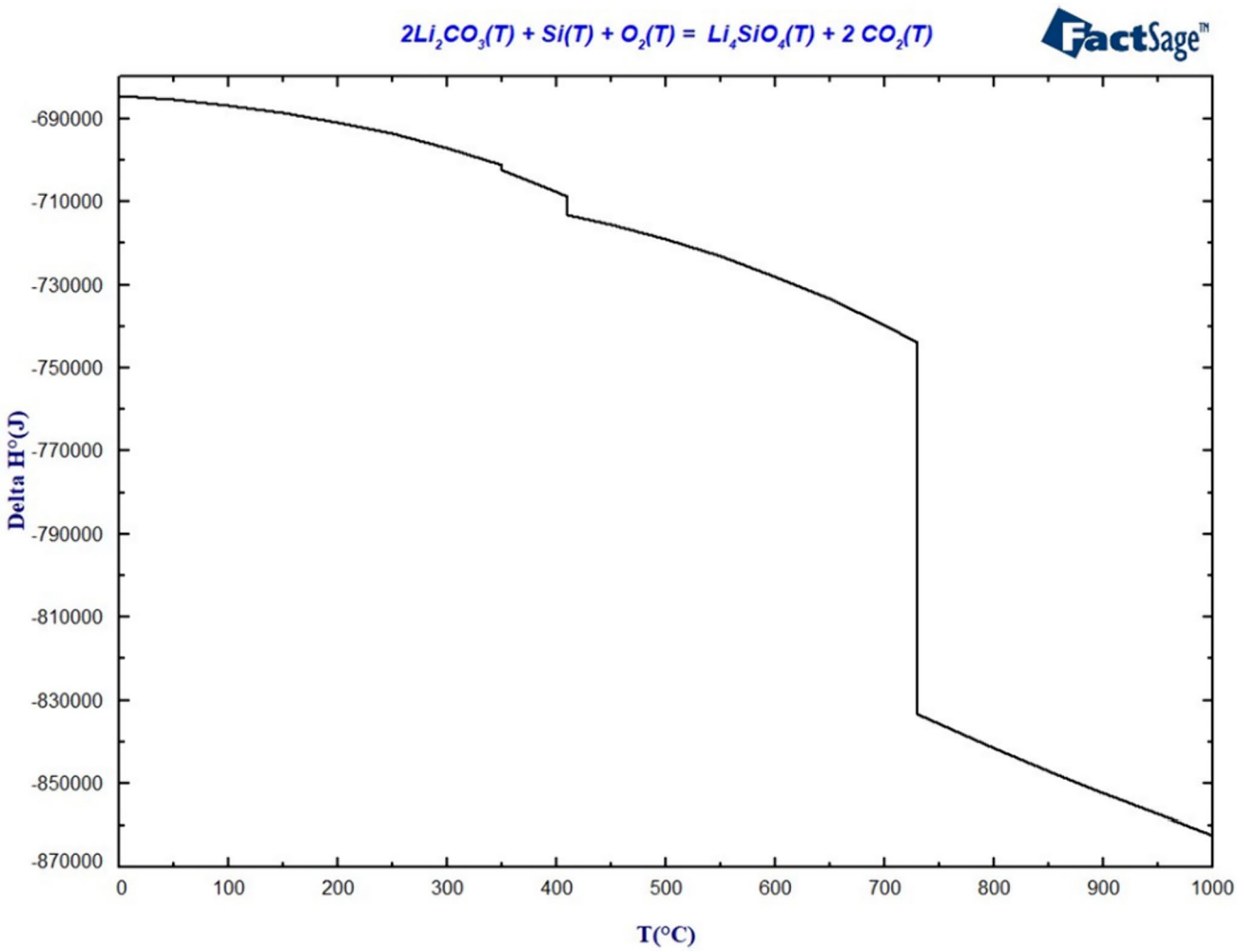


**Fig. 5** The enthalpy change of the combustion-assisted synthesis reaction

system to proceed in the direction of $Li_4SiO_4$ transformation and reduces the temperature of the system from 800 °C to 598 °C. These findings support the endothermic character of the solid-state synthesis. It was also found that the exothermic character of the combustion-assisted synthesis reaction is due to the combustion of silicon with oxygen. In other words, the exothermic energy required for the self-propagating $Li_4SiO_4$ conversion in the combustion-assisted synthesis reaction is initially provided by the reaction of silicon with oxygen. When the system is heated to 800 °C, the temperature rises to 2874 °C as a result of $Si + O_2 = SiO_2$ reaction as a first step, then $Li_2CO_3$ and $SiO_2$ use this heat to react. Thus, $Li_4SiO_4$ transformation takes place and the temperature of the system decreases to 2049 °C.

Simulations of the production of $Li_4SiO_4$ by solid state synthesis and combustion-assisted synthesis are shown in Figs. 7 and 8, respectively. The simulations performed for both production methods showed similar results. When the temperature of the starting mixture reaches 200 °C, $Li_2CO_3$ and $SiO_2$ react to form $Li_2Si_2O_5$. When the temperature is 250 °C, $SiO_2$ is depleted and $Li_2CO_3$ reacts with $Li_2Si_2O_5$ to form $Li_2SiO_3$. When the temperature reaches 350 and 400 °C respectively, $Li_2CO_3$ exhibits polymorphic transformation twice. $Li_2SiO_3$ formed at 250 °C and $Li_2CO_3$ formed at 400 °C react at 700 °C to form $Li_4SiO_4$.

The main difference between the two production methods is the different source of silicon used in the starting mixture. While $SiO_2$ is used as the silicon source in solid-state synthesis, metallic Si is used in combustion-assisted synthesis. Although production simulations have shown similar results, the use of metallic Si turns the production of $Li_4SiO_4$ into an exothermic character.

## Evaluation of Synthesis Route

In the combustion-assisted synthesis experiments, combustion synthesis was carried out according to reaction (1). The theoretical weight loss according to reaction (1)

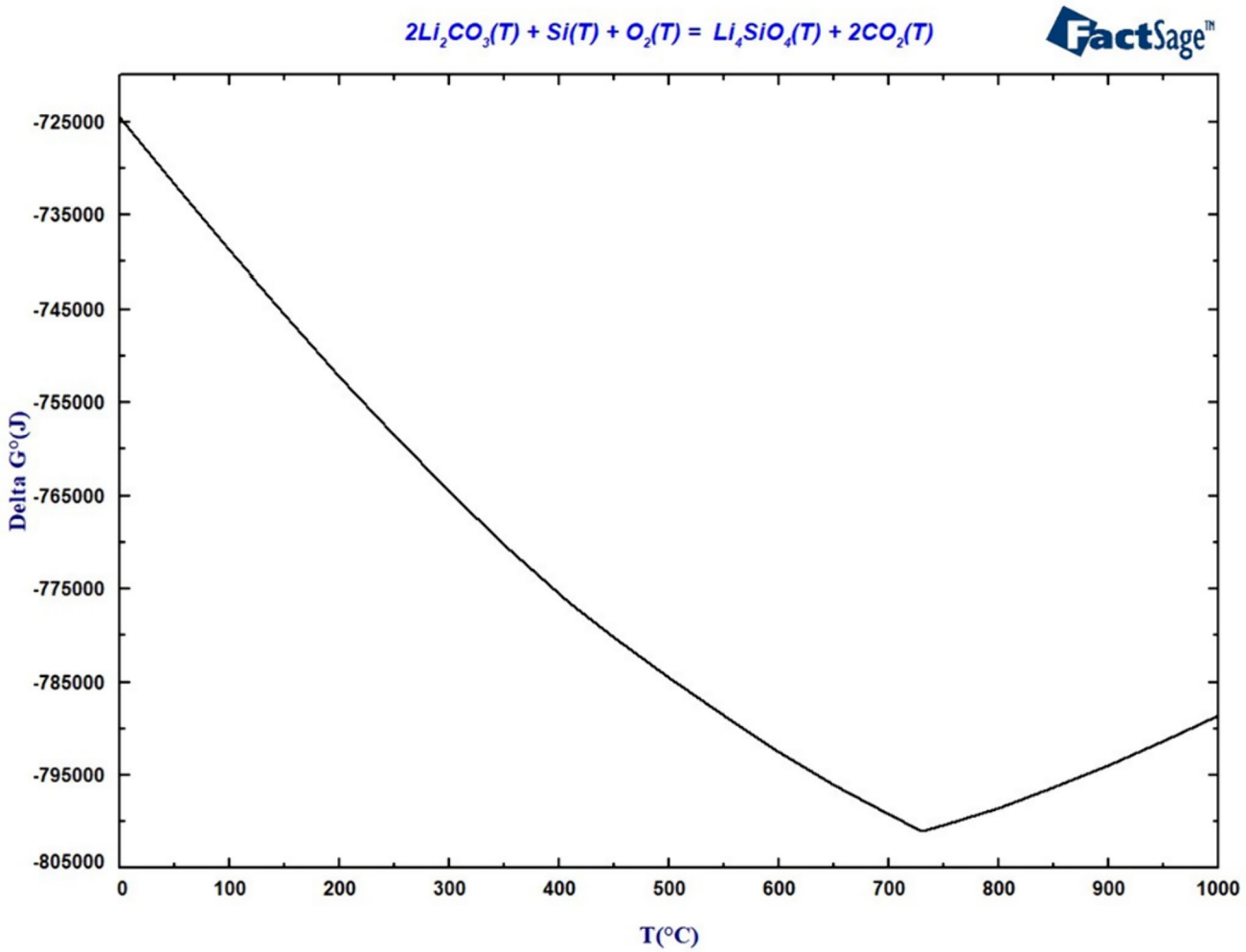


**Fig. 6** The Gibbs free energy change of the combustion-assisted synthesis reaction

was calculated as 31.85%, in other words, the weight of the product obtained at the end of the reaction should theoretically be 68.15% of the total weight of the reacted raw materials. The graph showing the remaining product weight ratios for the combustion-assisted synthesis experiments is given in Fig. 9. It is understood that the combustion synthesis reactions could not proceed and therefore the remaining product weight ratios were high in the preliminary experiments, which were carried out for 60 min and completed at synthesis temperatures lower than 700 °C. With increasing synthesis temperature, the residual product weight ratios decreased. Similarly, the large decrease in the remaining product weight ratio at 700 °C indicates that the conversion during combustion synthesis is largely complete and that the synthesis temperature of 700 °C is a critical temperature for reaction (1). This finding is in agreement with the thermodynamic simulation results and supported by the quantitative phase analysis results given below.

The variation of the residual product weight fraction is very small between 700 and 900 °C and is very close to the theoretically calculated value of 68.15%, especially from 850 °C onwards. Thus, it can be concluded that reaction (1) reached equilibrium at 850 °C for synthesis times of 45 min, 60 min and 75 min.

The XRD patterns of the combustion-assisted synthesis products are shown in Figs. 10, 11 and 12 for 60, 45 and 75 min. of synthesis duration respectively. With these XRD results, the effect of different synthesis temperatures on the phase formations of the synthesis products was evaluated.

In order to determine the temperature at which the conversion during reaction (1) would be largely complete, synthesis trials were carried out between 500 and 700 °C for 60 min. When the XRD patterns of the products obtained from these preliminary experiments are examined, it is seen that the synthesis reaction did not proceed at 500 and 550 °C and the products consisted of $Li_2CO_3$ (ICDD no: 01-087-0729) and Si (ICDD no: 01-075-0589) phases. When the

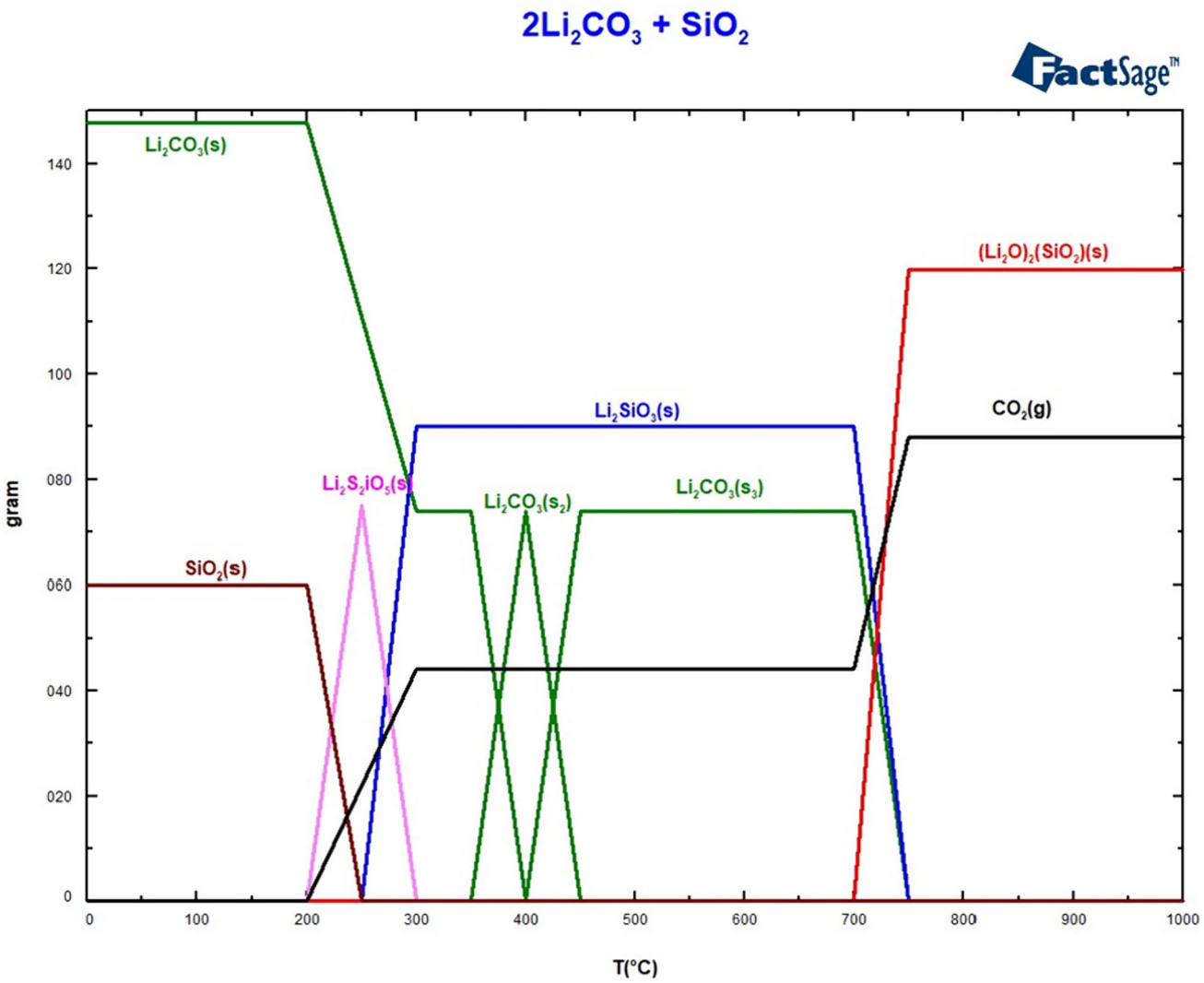


**Fig. 7** The modeling of $Li_4SiO_4$ production by solid-state synthesis reaction

combustion synthesis was completed at 600 °C, the main phases in the product formed were $Li_2CO_3$ and Si, but a very small amount of $Li_4SiO_4$ (ICDD no: 01-076-1085) was observed. When the synthesis temperature is increased up to 675 °C, it can be seen that the main phases in the products are still $Li_2CO_3$ and Si, but the amount of $Li_4SiO_4$ phase formed increases with increasing temperature. A very small amount of $Li_2SiO_3$ (ICDD no: 01-070-0330) was also formed at 675 °C. When the combustion synthesis is carried out at 700 °C and higher temperatures, it can be seen that the dominant phase in the products is $Li_4SiO_4$, with the presence of a small amount of $Li_2CO_3$. When the synthesis temperature is increased to 800 °C and above, the dominance of the $Li_4SiO_4$ phase increases further and the amount of $Li_2CO_3$ decreases. At 900 °C, a very small amount of $Li_2SiO_3$ phase is observed again.

According to the XRD results of the synthesis products with 60 min. duration, the transformation in reaction (1) was largely complete under the conditions of synthesis carried out at temperatures of 700 °C and higher. These XRD results are supported by the weight loss results given above and the quantitative phase analysis results given below.

As a result of the combustion-assisted synthesis experiments carried out in the muffle furnace for 60 min, it was determined that the critical temperature at which the conversion was largely complete for reaction (1) was 700 °C. Based on this result, the other combustion-assisted synthesis experiments were carried out at 700 °C and higher temperatures.

When the XRD results of the synthesis products with 45 min. duration, which proceeded according to reaction (1), are examined, it is seen that the dominant phase for each temperature is $Li_4SiO_4$. Again, there is a small amount

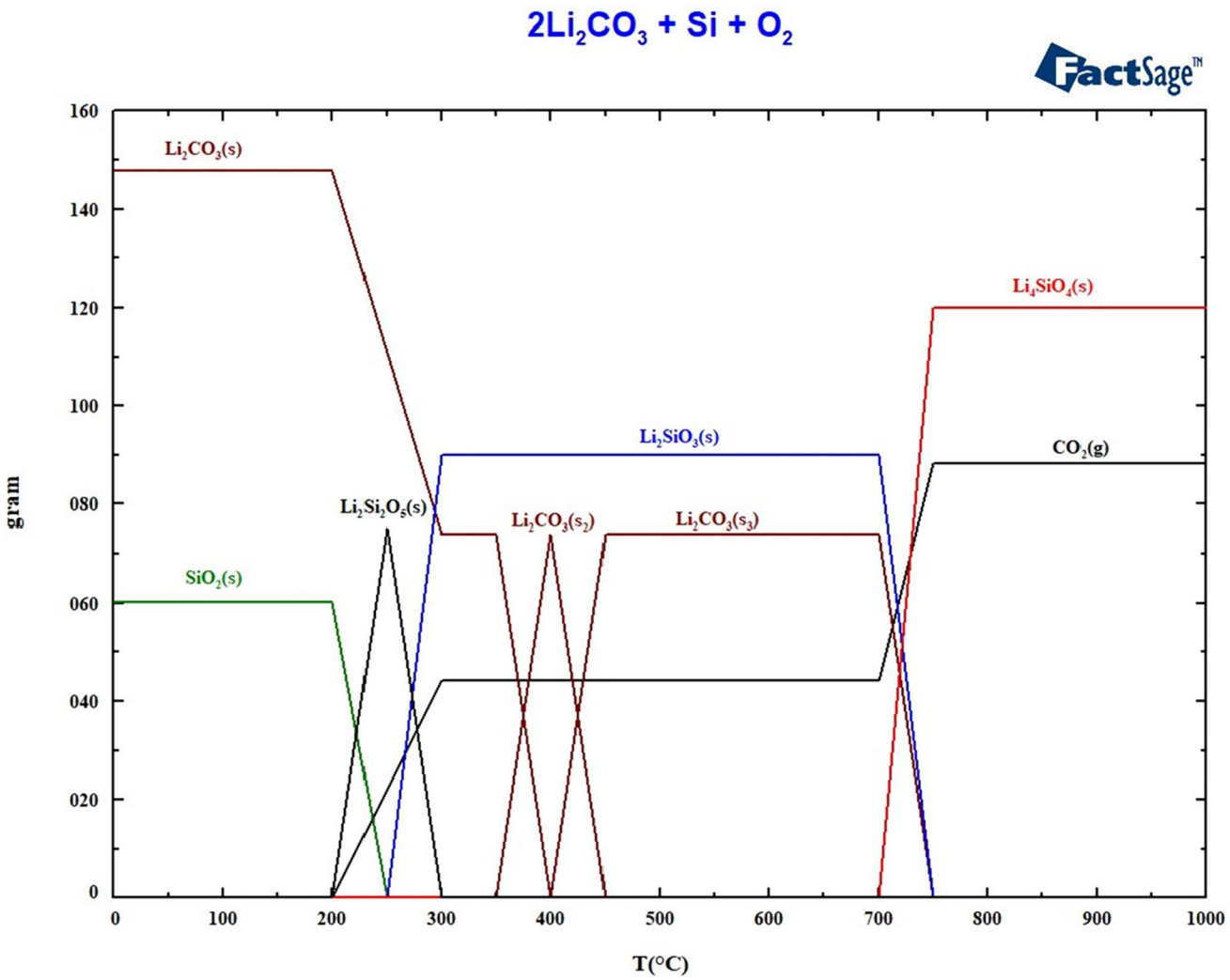


**Fig. 8** The modeling of $Li_4SiO_4$ production by combustion-assisted synthesis reaction

of $Li_2CO_3$ and very small amounts of Si and $SiO_2$ phases at each temperature. As the temperature increases, the dominance of $Li_2CO_3$ phase decreases. The $Li_2SiO_3$ phase, in very small amounts, is observed at 700, 750 °C, but not at 800, 850 °C, but again at 900 °C. These results are in agreement with the weight loss results and quantitative phase analysis results.

The results of the synthesis products with 75 min. duration according to reaction (1) were similar to the XRD results of the synthesis products with 45 and 60 min. duration. The dominant phase at all temperatures was $Li_4SiO_4$, while very small amounts of $Li_2CO_3$, Si and $SiO_2$ phases were observed. $Li_2SiO_3$ phase was observed only at 900 °C. As the temperature increased, the dominance of $Li_4SiO_4$ phase increased. Again, these results are consistent with the weight loss and quantitative phase analysis results.

$Li_4SiO_4$ content of the products obtained as a result of combustion-assisted synthesis experiments was determined by Rietveld refinement method. The $Li_4SiO_4$ phase percentages of the synthesis products are given in Fig. 13. Considering the amount of $Li_4SiO_4$ phase formed after the reaction, it is understood that the synthesis temperature of 700 °C is a critical temperature. In the experiments completed at temperatures lower than this temperature, the conversion could not be completed and reaction (1) could not reach the equilibrium state. The change in the $Li_4SiO_4$ phase percentages of the products is very small from 800 °C onwards. A careful examination of the graph shows that the highest $Li_4SiO_4$ phase percentage value was obtained at 850 °C, while this value decreased slightly at 900 °C. This can be explained by the sublimation of lithium oxide in $Li_2O$ form. Thermodynamic modeling also supports this sublimation. When the combustion synthesis was completed at 900 °C, a small amount of $Li_4SiO_4$ decomposed to $Li_2SiO_3$ according to the following reaction (2) [31, 32].

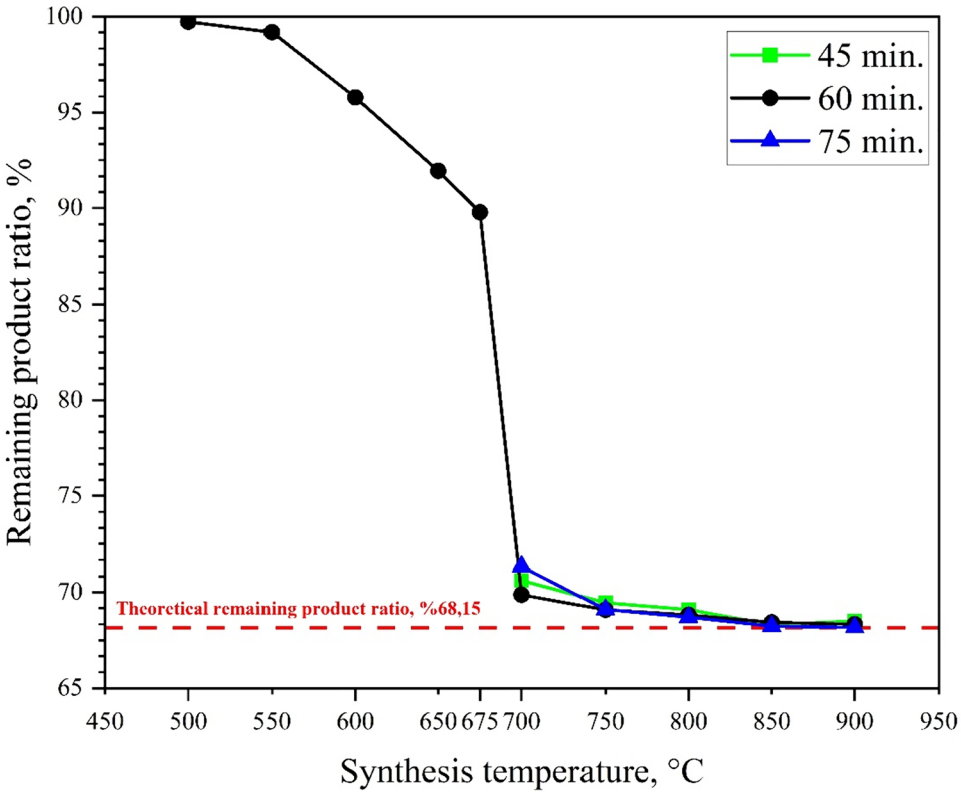


**Fig. 9** The remaining product weight ratios for the combustion-assisted synthesis experiments

$$Li_4SiO_4 \xrightarrow{T} Li_2SiO_3 + Li_2O \quad (2)$$

$Li_4SiO_4$ crystallite size values of the synthesis products are given in Fig. 14. When the graph was analyzed, it was observed that the crystallite size values of the resulting products increased as the synthesis temperature and duration increased. Among the synthesis products, the product with the lowest crystallite size value of 126.58 nm was obtained at 700 °C and 45 min. synthesis conditions. The largest crystallite size belongs to the product obtained at 900 °C and 75 min. synthesis parameters and its value was calculated as 487.67 nm.

The crystallite size values of the combustion-assisted synthesis products are larger than the crystallite size values of the solid-state products given in literature. This is due to the high theoretical maximum temperature ($T_{ad}$) values reached during combustion depending on the inputs of the combustion assisted solid state reaction, as can be seen from the thermodynamic simulation results, and the slow cooling rate of the products obtained as a result of combustion assisted synthesis due to cooling in the muffle furnace. This slow cooling caused the $Li_4SiO_4$ crystals formed to grow.

The specific surface area values of the synthesis products are given in Fig. 15. Specific surface area measurements of synthesis products that exhibited insufficient conversion and were carried out at temperatures lower than 700 °C, were not performed.

As the synthesis temperature increased, the specific surface area values of the products decreased. The specific surface area values of the products obtained at 700 °C were measured as 4.975, 4.272 and 3.357 $m^2/g$, respectively, under experimental conditions where the synthesis time was 45, 60 and 75 min. The specific surface area values of the products obtained at 900 °C under the same experimental conditions were 2,128, 1,987 and 1,472 $m^2/g$, respectively. In the synthesis studies carried out at the same temperature, it was found that the specific surface area values of the products decreased as the synthesis duration increased. In the experimental conditions where the synthesis temperature was 800 °C and higher, it was observed that the specific surface area values of the products remained almost unchanged for each different synthesis duration.

The average particle size values of the synthesis products are given in Fig. 16. Particle size measurements of synthesis products with insufficient conversion and at temperatures lower than 700 °C were not performed.

The average particle size values of the products increase with increasing synthesis temperature. In the experimental conditions where the synthesis temperature was between 700 and 850 °C, the increase in the average particle size of the products obtained for each different synthesis duration was

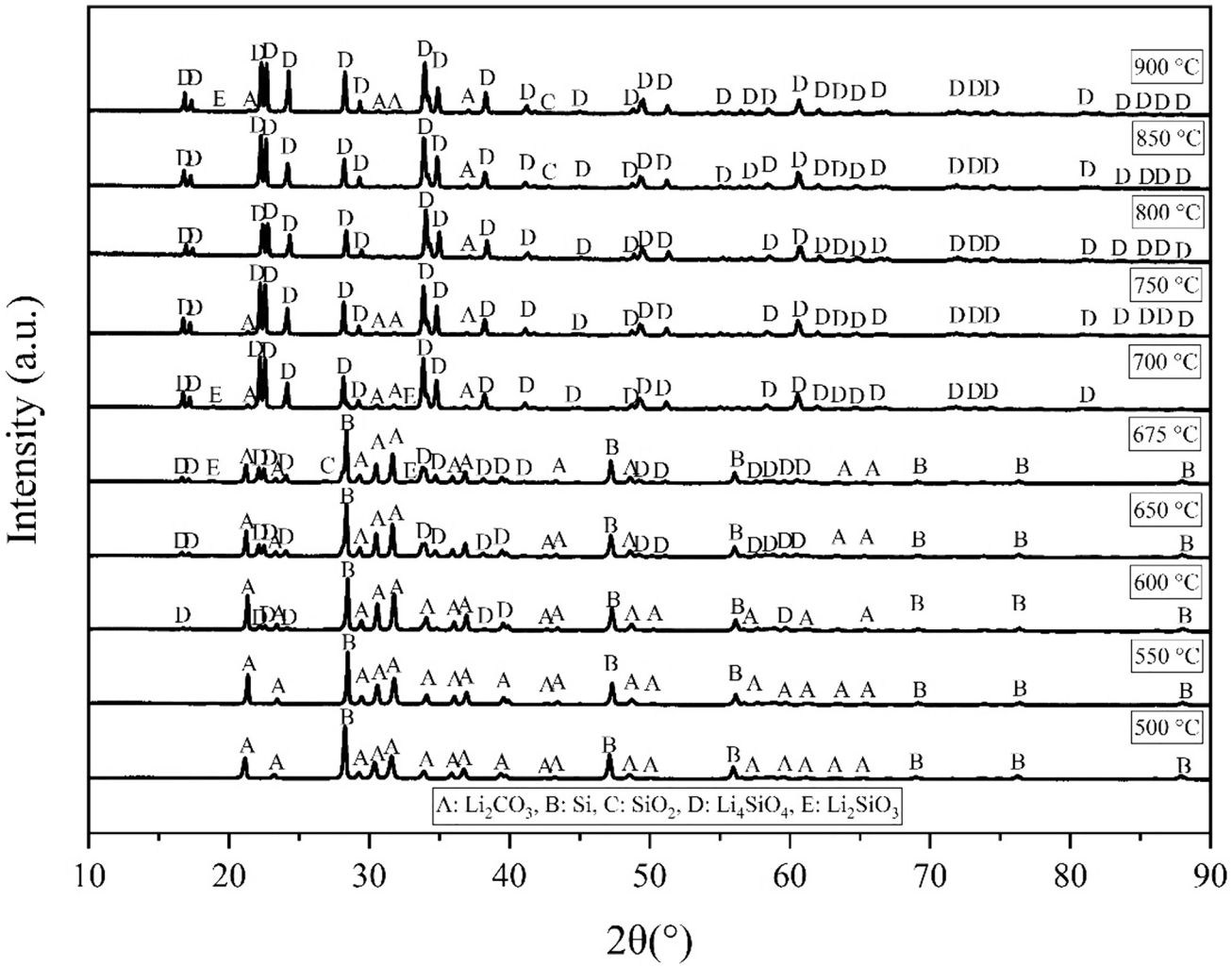


**Fig. 10** XRD patterns of the combustion-assisted synthesis products with 60 min. synthesis duration

very small. When the temperature was increased to 900 °C, the increase in the average particle size of the synthesis products became very significant. Similarly, the average particle size values of the products increased with increasing synthesis duration. This increase was very small for the products of synthesis experiments conducted at 700, 750, 800 and 850 °C. However, there was a significant increase in the average particle size of the products obtained as a result of synthesis experiments conducted at 900 °C from 45 to 75 min.

SEM micrographs of the synthesis products are shown in Fig. 17. When the images of the synthesis products were examined, it was determined that the particle size was approximately 10 µ. SEM micrographs showed consistency with the specific surface area and particle size measurement results.

## Results of $CO_2$ Sorption Tests

The conditions in the $CO_2$ capture experiments with $Li_4SiO_4$ powders performed in this study were also modeled with FactSage 8.2 software using the equilibrium module. The simulation of $CO_2$ capture of $Li_4SiO_4$ under a gas mixture of 92% $CO_2$ and 8% $N_2$ by volume is shown in Fig. 18. Theoretically, $Li_4SiO_4$ captures $CO_2$ up to 600 °C according

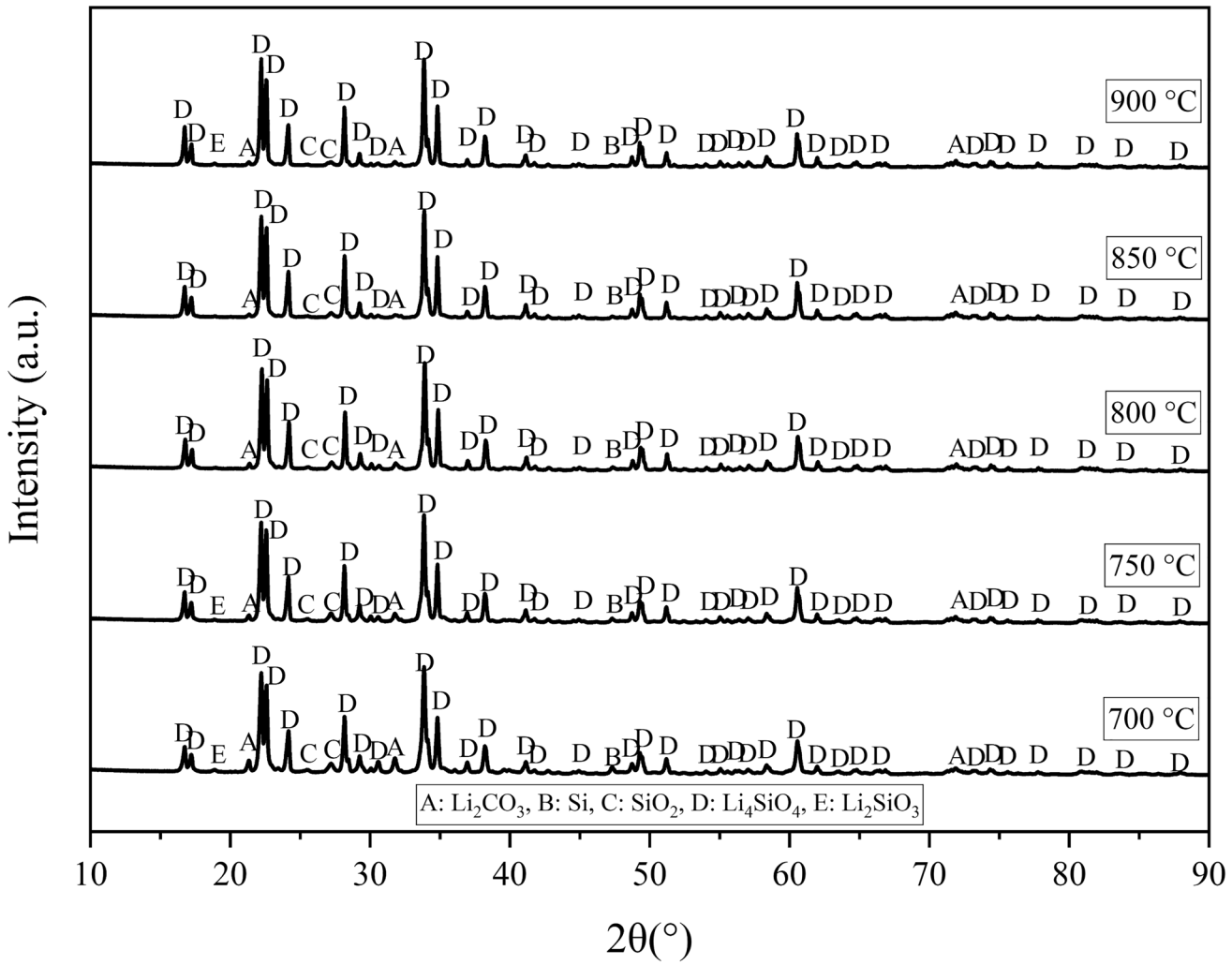


**Fig. 11** XRD patterns of the combustion-assisted synthesis products with 45 min. synthesis duration

to the reversible reaction (3) given below with a maximum theoretical capture capacity of 36.7 wt% and regenerates after this temperature [5, 17, 33, 34].

$$Li_4SiO_4 + CO_2 \leftrightarrow Li_2SiO_3 + Li_2CO_3 \quad (3)$$

In addition, as stated in the literature, it has been determined that as the $CO_2$ partial pressure in the environment decreases, the amount of $CO_2$ to be captured by $Li_4SiO_4$ will decrease [35].

The products obtained from the synthesis studies were subjected to $CO_2$ capture test under 92% $CO_2$ gas atmosphere. The maximum amount of $CO_2$ captured by the synthesis products at the end of 120 min is given in Fig. 19. In Fig. 20., $CO_2$ capture performances based on characterized physical properties are also presented. In this way, it is aimed to establish a relationship between the $CO_2$ capture performance of the products and the physical properties of the products.

When the $CO_2$ capture performances of the synthesis products were examined, it was observed that they performed far below the theoretical maximum $CO_2$ capture value of 36.7% (0.367 g $CO_2$/1 g sorbent) for pure $Li_4SiO_4$ [23]. The synthesis products had $CO_2$ capture values ranging between 4.79 and 12.80%. The products obtained as a result of combustion-assisted synthesis did not show good $CO_2$

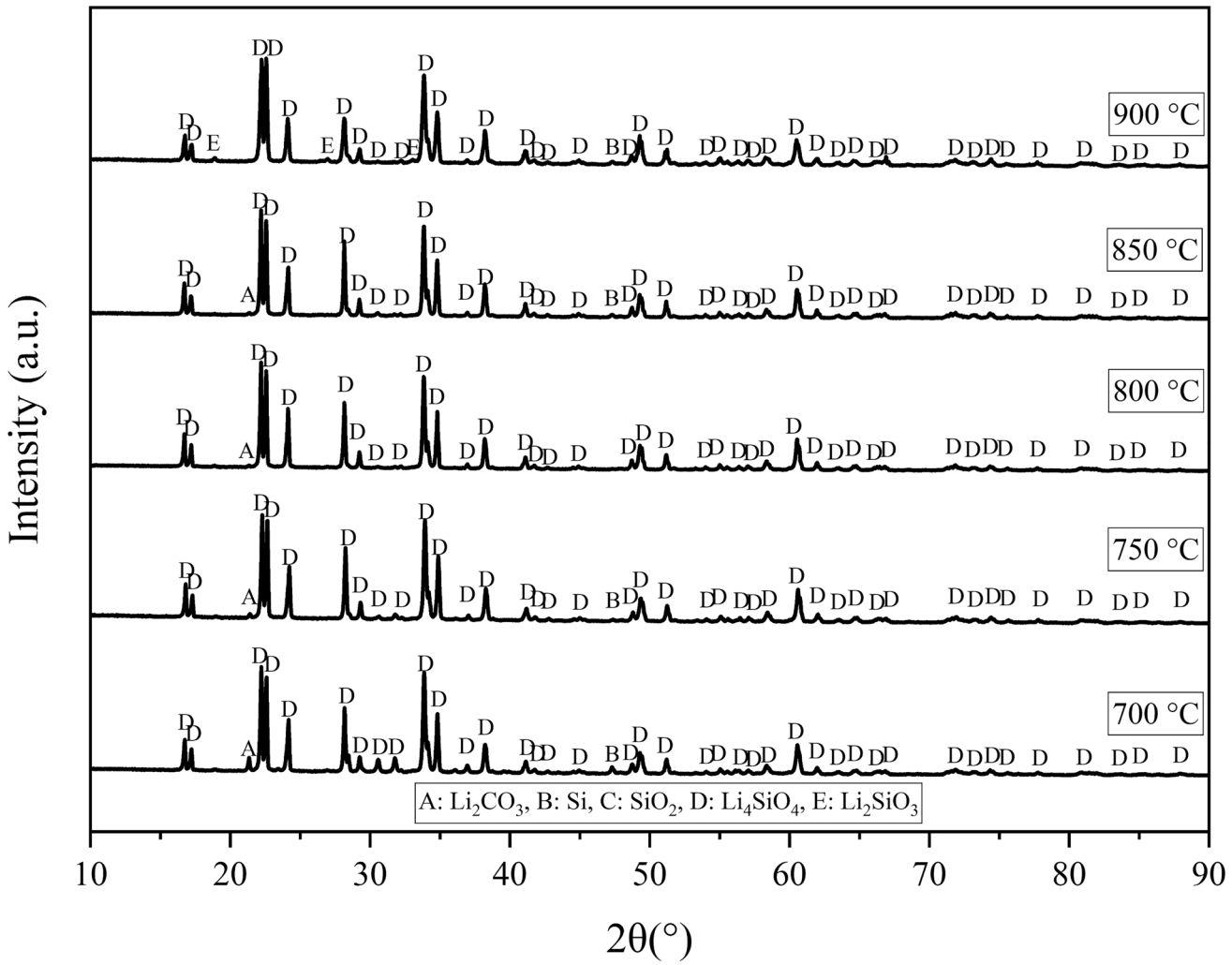


**Fig. 12** XRD patterns of the combustion-assisted synthesis products with 75 min. synthesis duration

capture performance despite their high $Li_4SiO_4$ content. Based on these results, it was determined that in order for these products to approach the theoretical maximum $CO_2$ capture values, it is necessary for them to have certain characteristic properties in addition to having high $\%Li_4SiO_4$ phase percentage. These characteristics have been reported in our previous study [36].

The graph showing the maximum $CO_2$ capture values according to the physical properties of the products. When the physical properties of product number 16, which has a maximum $CO_2$ capture value of 12.80%, are examined, it is seen that although the $\%Li_4SiO_4$ phase percentage value is lower than the other products, it has the lowest crystallite size value, the highest specific surface area value and the lowest average particle size value. Again, when the graph is analyzed, it is determined that $CO_2$ capture performance decreases as the average particle size values increase, while $CO_2$ capture performance increases as the specific surface area values increase.

In line with these results and the information given above, it has been revealed that in order to obtain a good $CO_2$ capture performance, high conversion rate and high $\%Li_4SiO_4$ phase content value alone will not be sufficient, but the sorbent material should have low average particle size, high specific surface area and low crystallite size values.

All the characterization results of the products are summarized in Table 2 below. When the synthesis duration

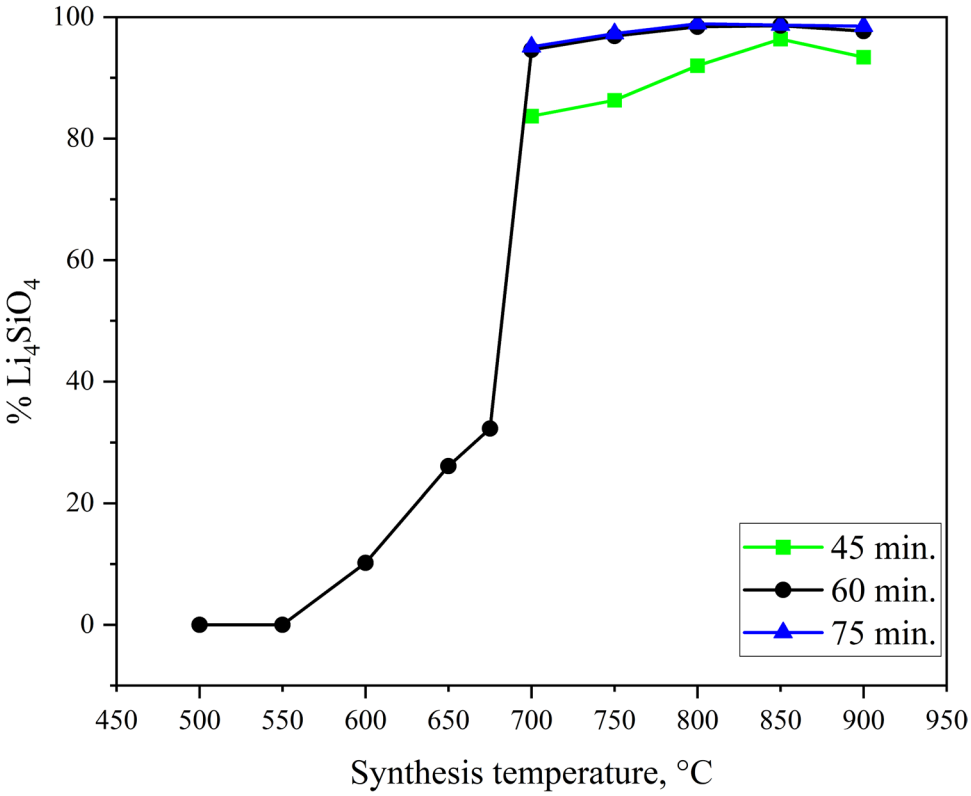


**Fig. 13** $Li_4SiO_4$ content of the products

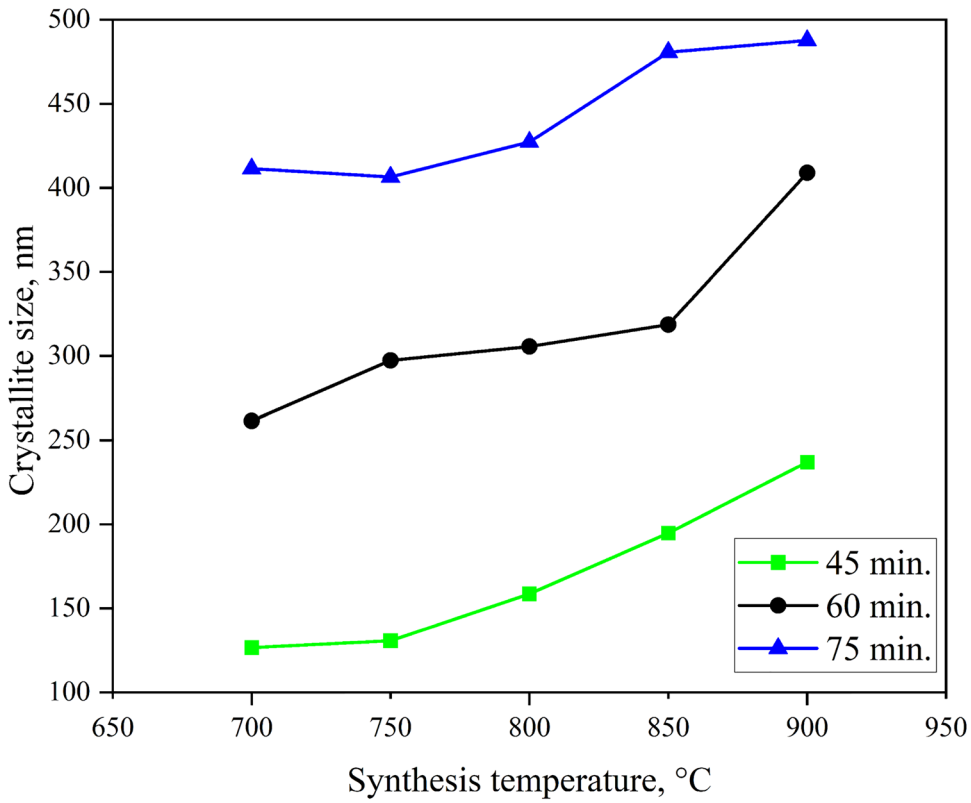


**Fig. 14** $Li_4SiO_4$ crystallite size values of the synthesis products

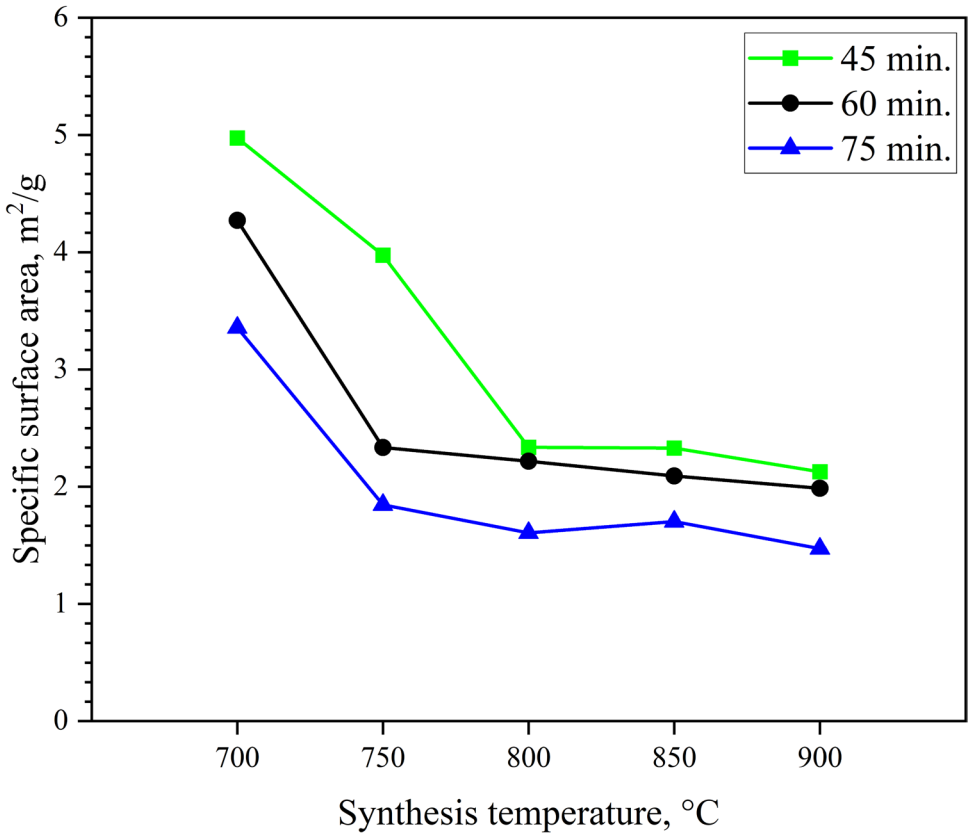


**Fig. 15** The specific surface area values of the synthesis products

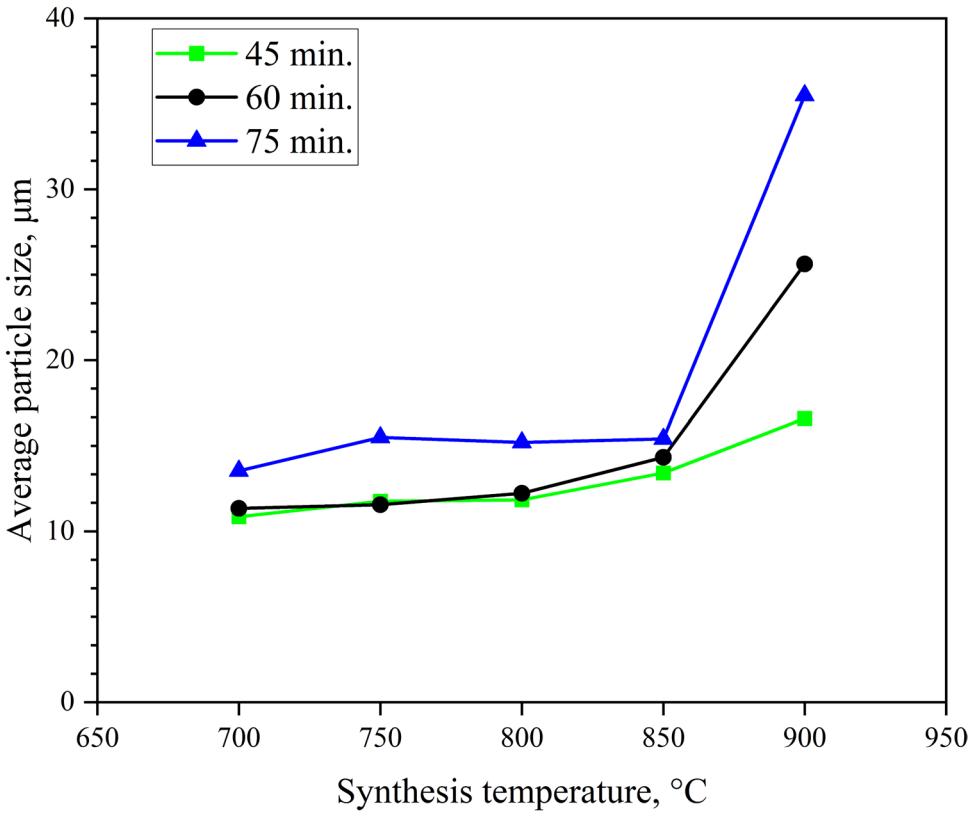


**Fig. 16** The average particle size values of the synthesis products

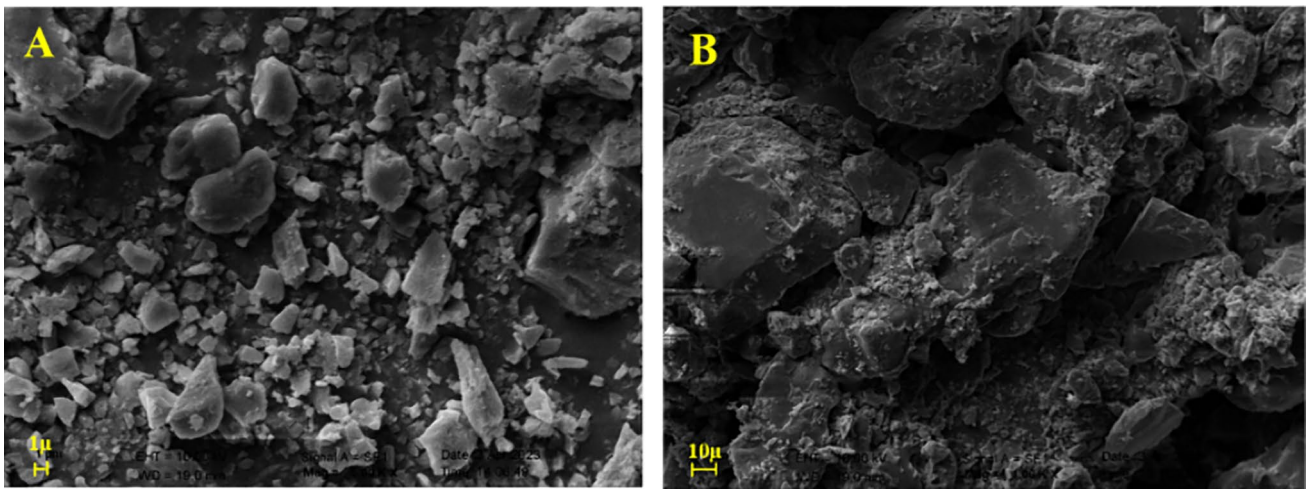


**Fig. 17** Morphologies of the synthesis products. (A:5000X, B:1000X)

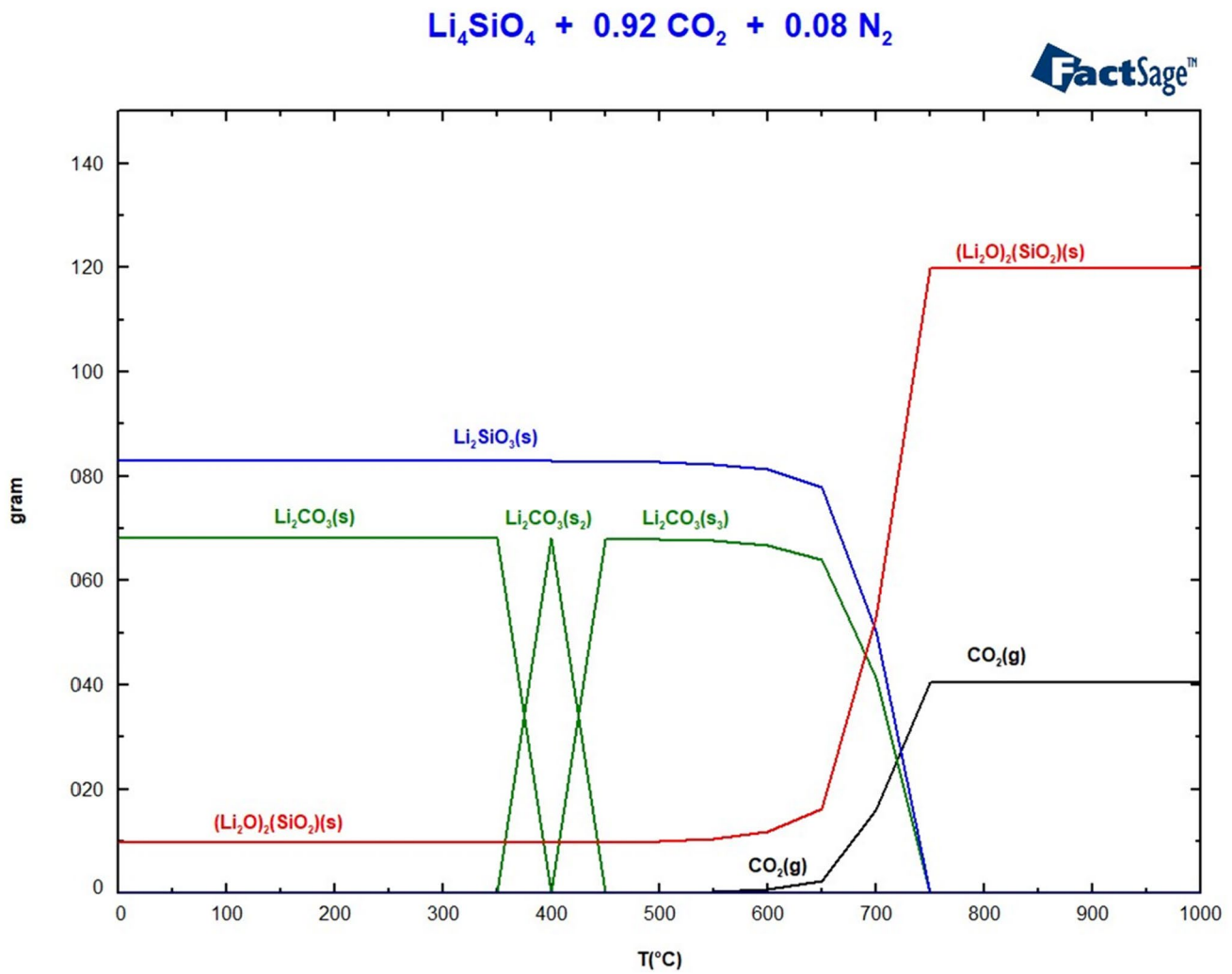


**Fig. 18** Simulation of $CO_2$ capture with $Li_4SiO_4$ (92% $CO_2$, 8% $N_2$ atmosphere)

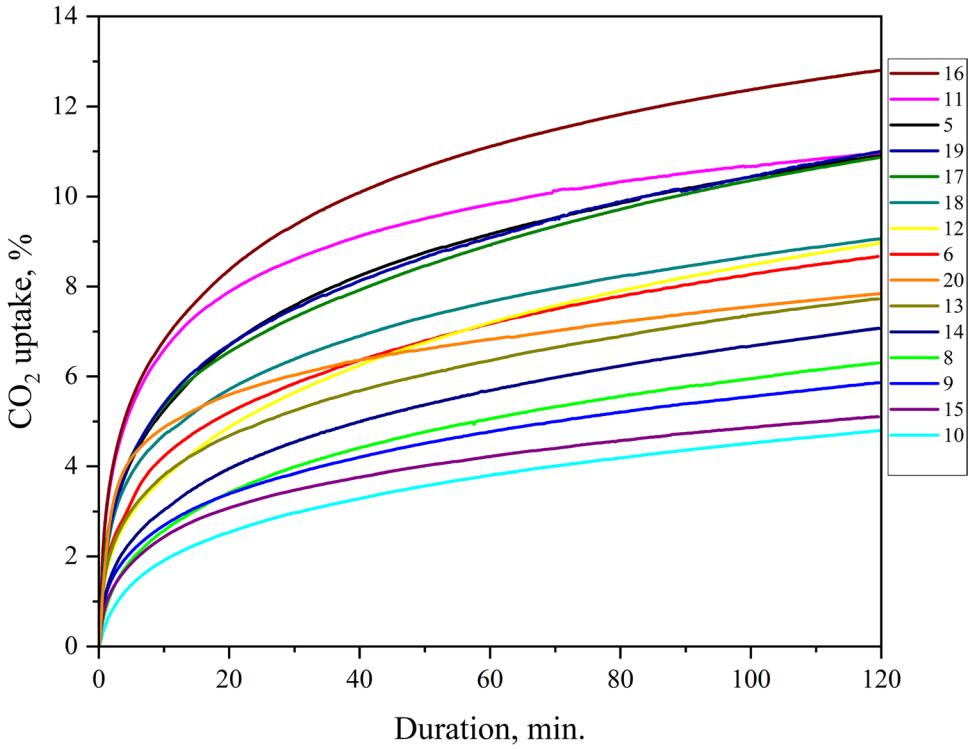


**Fig. 19** $CO_2$ capture performances of the products

was kept constant, it was found that the crystallite size and average particle size values increased with increasing synthesis temperature, while the specific surface area values decreased. Similarly, when the synthesis temperature was kept constant, it was observed that the crystallite size and average particle size values increased with increasing synthesis duration, while the specific surface area value decreased.

## Conclusions

In this study, $Li_4SiO_4$ powders used as $CO_2$ capture sorbents were produced by combustion-assisted synthesis. Prior to the synthesis studies, the reaction conditions were modeled with FactSage 8.2 software. Synthesis products were characterized by weight loss determination, phase analysis, quantitative phase analysis, crystallite size calculations, specific surface area measurement, particle size measurement and SEM.

Thermodynamic simulations completed prior to the synthesis studies revealed that the production of $Li_4SiO_4$ by combustion-assisted synthesis is possible at temperatures of 700 °C and higher if metallic Si is used as the silicon source.

The weight loss results showed that the conversion during synthesis takes place at temperatures of 700 °C and higher. This result is in agreement with the thermodynamic simulation results.

The values found by $Li_4SiO_4$ crystallite size calculations of the synthesis products ranged between 126.58 and 487.67 nm. It was found that the crystallite size values increased with increasing synthesis temperature and time. The synthesis product with the largest specific surface area value was synthesized at 700 °C and 45 min. It was determined that the specific surface area values decreased with increasing synthesis temperature and duration. The average particle size values increased with increasing synthesis temperature and duration.

The optimum production conditions for synthesis were determined as 850 °C and 60 min. considering the synthesis temperature, duration and $Li_4SiO_4$ content of the final product (98.6%).

As a result of $CO_2$ capture tests performed in a gas mixture containing 92% $CO_2$, it was found that the synthesis products showed a capture performance between 4.79 and 12.80%. This performance was far below the theoretical maximum capture capacity of $Li_4SiO_4$.

The production of $Li_4SiO_4$ powders by combustion-assisted synthesis method was realized for the first time in this study. Considering the $CO_2$ capture performance

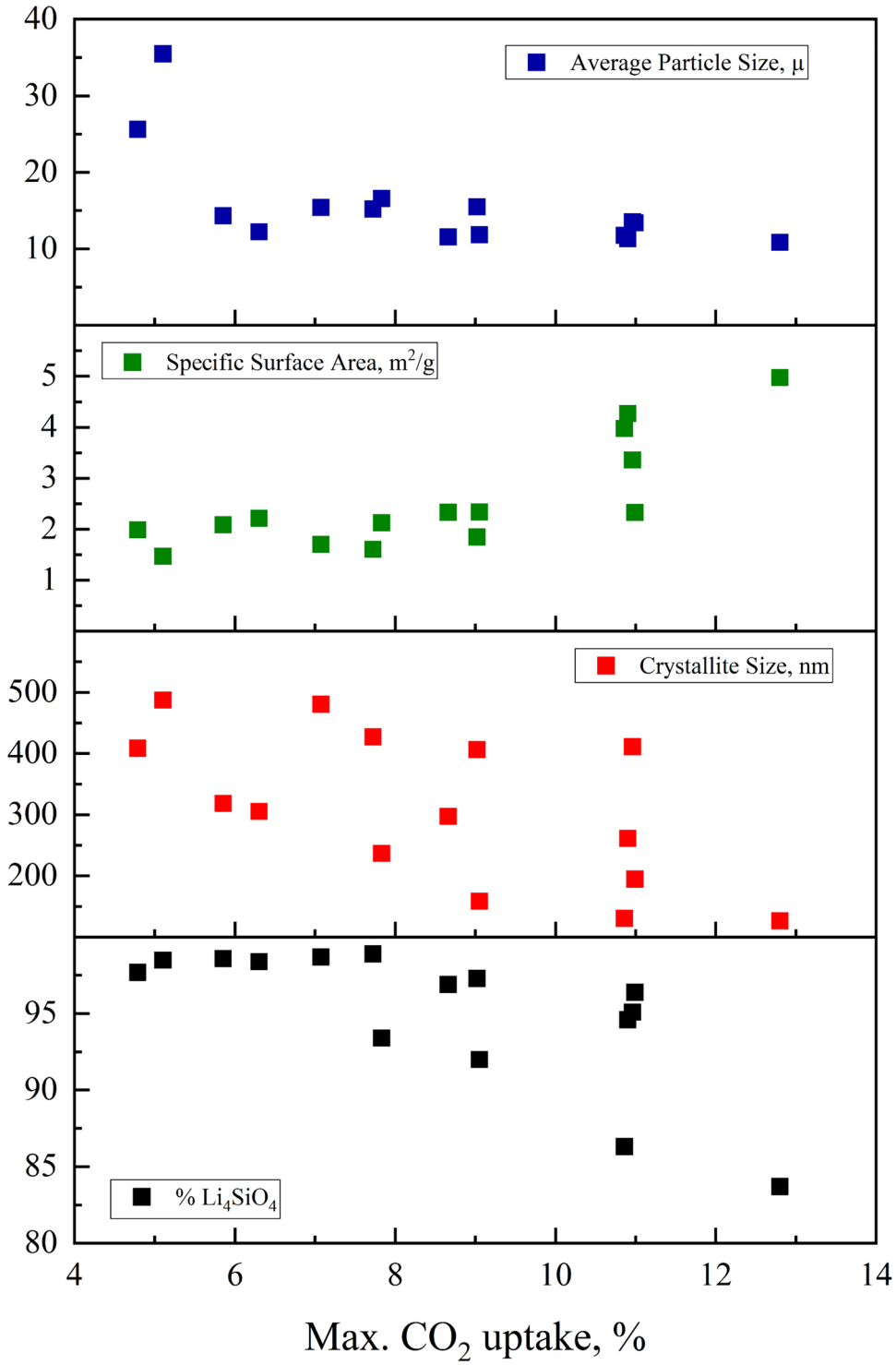


**Fig. 20** $CO_2$ capture performances based on characterized physical properties

of synthesis products, it is understood that modifications should be made in the properties of the products for performance improvement. It is a known fact that the properties of the final product in such processes are directly related to the raw material properties and process conditions. In this context, in order for the synthesis products to have smaller crystallite size, larger specific surface area and smaller particle size values, it is recommended to mix the synthesis raw materials $Li_2CO_3$ and Si powders with a ball mill and then complete the synthesis work. In order to prevent crystal growth after synthesis, another suggestion of this study is to remove the products from the muffle furnace as soon as the synthesis time is over and allow them to cool in an open atmosphere.

**Table 2** Characterization results of the products

| Exp. No | % $Li_4SiO_4$ | Crystallite size, nm | Specific surface area, $m^2/g$ | Average particle size, μm | Max. $CO_2$ uptake, % |
|---|---|---|---|---|---|
| 5 | 94.6 | 261.35 | 4.272 | 11.34 | 10.90 |
| 6 | 96.9 | 297.30 | 2.334 | 11.56 | 8.66 |
| 8 | 98.4 | 305.60 | 2.218 | 12.22 | 6.30 |
| 9 | 98.6 | 318.57 | 2.091 | 14.33 | 5.85 |
| 10 | 97.7 | 408.92 | 1.987 | 25.63 | 4.79 |
| 11 | 95.1 | 411.37 | 3.357 | 13.54 | 10.96 |
| 12 | 97.3 | 406.43 | 1.846 | 15.5 | 9.02 |
| 13 | 98.9 | 427.20 | 1.606 | 15.2 | 7.72 |
| 14 | 98.7 | 480.60 | 1.703 | 15.41 | 7.07 |
| 15 | 98.5 | 487.67 | 1.472 | 35.49 | 5.10 |
| 16 | 83.7 | 126.58 | 4.975 | 10.85 | 12.80 |
| 17 | 86.3 | 130.66 | 3.975 | 11.76 | 10.86 |
| 18 | 92.0 | 158.60 | 2.337 | 11.84 | 9.05 |
| 19 | 96.4 | 194.79 | 2.329 | 13.41 | 10.99 |
| 20 | 93.4 | 236.96 | 2.128 | 16.59 | 7.83 |

**Acknowledgements** This work is funded by the Scientific Research Projects Coordination Unit (BAP) at Istanbul Technical University [Project No: 42201]. Also, corresponding author sends special thanks to Dr. Maria Teresa Izquierdo from Instituto de Carboquimica, Zaragoza, Spain for the $CO_2$ uptake tests and characterization studies.

**Funding** Open access funding provided by the Scientific and Technological Research Council of Türkiye (TÜBİTAK).

## Declarations

**Conflict of interest** On behalf of all authors, the corresponding author states that there is no conflict of interest.



## References

1. Yoro KO, Daramola MO (2020) $CO_2$ emission sources, greenhouse gases, and the global warming effect. Elsevier, Amsterdam
2. Sekoai PT, Yoro KO (2016) Biofuel development initiatives in Sub-Saharan Africa: opportunities and challenges. Climate 4(2):33. https://doi.org/10.3390/CLI4020033
3. Kang Y, Khan S, Ma X (2009) Climate change impacts on crop yield, crop water productivity and food security – a review. Prog Nat Sci 19(12):1665–1674. https://doi.org/10.1016/J.PNSC.2009.08.001
4. Wang Y, Zhao L, Otto A, Robinius M, Stolten D (2017) A review of post-combustion $CO_2$ capture technologies from coal-fired power plants. Energy Proc 114:650–665. https://doi.org/10.1016/j.egypro.2017.03.1209
5. Chen S, Dai J, Qin C, Yuan W, Manovic V (2022) Adsorption and desorption equilibrium of $Li_4SiO_4$-based sorbents for high-temperature $CO_2$ capture. Chem Eng J 429:132236. https://doi.org/10.1016/J.CEJ.2021.132236
6. Dlugokencky E, Tans P. NOAA/GML. gml.noaa.gov/ccgg/trends/
7. Bobicki ER, Liu Q, Xu Z, Zeng H (2012) Carbon capture and storage using alkaline industrial wastes. Prog Energy Combust Sci 38(2):302–320. https://doi.org/10.1016/j.pecs.2011.11.002
8. IPCC (2005) Carbon dioxide capture and storage. IPCC, Cambridge
9. Lee ZH, Lee KT, Bhatia S, Mohamed AR (2012) Post-combustion carbon dioxide capture: evolution towards utilization of nanomaterials. Renew Sustain Energy Rev 16(5):2599–2609. https://doi.org/10.1016/j.rser.2012.01.077
10. Leung DYC, Caramanna G, Maroto-Valer MM (2014) An overview of current status of carbon dioxide capture and storage technologies. Renew Sustain Energy Rev 39(November):426–443. https://doi.org/10.1016/j.rser.2014.07.093
11 Rochelle GT (2009) Amine scrubbing for $CO_2$ capture. Science 325(5948):1652–1654. https://doi.org/10.1126/science.1176731
12. Mondal MK, Balsora HK, Varshney P (2012) Progress and trends in $CO_2$ capture/separation technologies: a review. Energy 46(1):431–441. https://doi.org/10.1016/j.energy.2012.08.006
13. Gray ML, Champagne KJ, Fauth D, Baltrus JP, Pennline H (2008) Performance of immobilized tertiary amine solid sorbents for the capture of carbon dioxide. Int J Greenh Gas Control 2(1):3–8. https://doi.org/10.1016/S1750-5836(07)00088-6
14. Rao GJ, Mazumder R, Bhattacharyya S, Chaudhuri P (2017) Synthesis, $CO_2$ absorption property and densification of $Li_4SiO_4$ powder by glycine-nitrate solution combustion method and its comparison with solid state method. J Alloys Compd 725:461–471. https://doi.org/10.1016/J.JALLCOM.2017.07.163
15. Shan S, Jia Q, Jiang L, Li Q, Wang Y, Peng J (2013) Novel $Li_4SiO_4$-based sorbents from diatomite for high temperature $CO_2$ capture. Ceram Int 39(5):5437–5441. https://doi.org/10.1016/j.ceramint.2012.12.051
16. Hu Y, Liu W, Zhou Z, Yang Y (2018) Preparation of $Li_4SiO_4$ sorbents for carbon dioxide capture via a spray-drying technique. Energy Fuels 32(4):4521–4527. https://doi.org/10.1021/acs.energyfuels.7b03051
17 Zhang Y, Gao Y, Louis B, Wang Q, Lin W (2019) Fabrication of lithium silicates from zeolite for $CO_2$ capture at high temperatures. J Energy Chem. https://doi.org/10.1016/j.jechem.2018.08.014
18. Hu Y, Liu L, Liu W, Zhou Z (2021) Structurally improved $Li_4SiO_4$ sorbents derived from lithium salicylate precursor for enhanced $CO_2$ capture. Fuel Process Technol 224:107027. https://doi.org/10.1016/J.FUPROC.2021.107027
19. Li F, Wang Y, Liu K, Wu Y, Ai J, Zhang J (2022) Preparation of $Li_4SiO_4$-based adsorbents with coal slag for high temperature cyclic $CO_2$ capture. Fuel 310:121687. https://doi.org/10.1016/J.FUEL.2021.121687
20. Pfeiffer H, Bosch P, Bulbulian S (1998) Synthesis of lithium silicates. J Nucl Mater 257(3):309–317. https://doi.org/10.1016/S0022-3115(98)00449-8
21. Kim H, Jang HD, Choi M (2015) Facile synthesis of macroporous $Li_4SiO_4$ with remarkably enhanced $CO_2$ adsorption kinetics. Chem Eng J 280:132–137. https://doi.org/10.1016/J.CEJ.2015.05.127

22. Izquierdo MT, Turan A, García S, Maroto-Valer MM (2018) Optimization of $Li_4SiO_4$ synthesis conditions by a solid state method for maximum $CO_2$ capture at high temperature. J Mater Chem A 6(7):3249–3257. https://doi.org/10.1039/c7ta08738a
23. Izquierdo MT, Gasquet V, Sansom E, Ojeda M, Garcia S, Maroto-Valer MM (2018) Lithium-based sorbents for high temperature $CO_2$ capture: effect of precursor materials and synthesis method. Fuel 230:45–51. https://doi.org/10.1016/j.fuel.2018.05.041
24. Mandal D, Jadeja MC, Chougule BK (2017) Synthesis of lithium orthosilicate and fabrication of pebbles by the solid-state reaction process. Indian Chem Eng 59(1):21–30. https://doi.org/10.1080/00194506.2015.1064790
25. Venegas MJ, Fregoso-Israel E, Escamilla R, Pfeiffer H (2007) Kinetic and reaction mechanism of $CO_2$ sorption on $Li_4SiO_4$: Study of the particle size effect. Ind Eng Chem Res 46(8):2407–2412. https://doi.org/10.1021/ie061259e
26. Varma A, Mukasyan AS (2004) Combustion synthesis of advanced materials: fundamentals and applications. Korean J Chem Eng 21(2):527–536. https://doi.org/10.1007/BF02705444
27. Moore JJ, Feng HJ (1995) Combustion synthesis of advanced materials: Part I. Reaction parameters. Prog Mater Sci 39(4–5):243–273. https://doi.org/10.1016/0079-6425(94)00011-5
28. Kingsley JJ, Suresh K, Patil KC (1990) Combustion synthesis of fine-particle metal aluminates. J Mater Sci 25(2):1305–1312. https://doi.org/10.1007/BF00585441
29. Gorinta J, Choudhary A, Bhattacharyya S, Chaudhuri P, Mazumder R (2012) Synthesis of lithium orthosilicate by solution combustion technique and its microwave sintering. Trans Indian Ceram Soc 71(4):229–231. https://doi.org/10.1080/0371750X.2013.772743
30. Bale CW et al (2016) FactSage thermochemical software and databases, 2010–2016. Calphad Comput Coupling Phase Diagrams Thermochem 54:35–53. https://doi.org/10.1016/j.calphad.2016.05.002
31. Shan S, Li S, Jia Q, Jiang L, Wang Y, Peng J (2013) Impregnation precipitation preparation and kinetic analysis of $Li_4SiO_4$-based sorbents with fast $CO_2$ adsorption rate. Ind Eng Chem Res 52(21):6941–6945. https://doi.org/10.1021/ie400743p
32. Cruz D, Bulbulian S, Lima E, Pfeiffer H (2006) Kinetic analysis of the thermal stability of lithium silicates ($Li_4SiO_4$ and $Li_2SiO_3$). J Solid State Chem 179(3):909–916. https://doi.org/10.1016/J.JSSC.2005.12.020
33. Pan Y, Zhang Y, Zhou T, Louis B, O'Hare D, Wang Q (2017) Fabrication of lithium silicates as highly efficient high-temperature $CO_2$ sorbents from SBA-15 Precursor. Inorg Chem 56(14):7821–7834. https://doi.org/10.1021/acs.inorgchem.7b00559
34. Essaki K, Kato M, Nakagawa K (2006) $CO_2$ removal at high temperature using packed bed of lithium silicate pellets. J Ceram Soc Japan 114(1333):739–742. https://doi.org/10.2109/jcersj.114.739
35. Hedin N, Andersson L, Bergström L, Yan J (2013) Adsorbents for the post-combustion capture of $CO_2$ using rapid temperature swing or vacuum swing adsorption. Appl Energy 104:418–433. https://doi.org/10.1016/j.apenergy.2012.11.034
36. Benzesik K, Turan A, Sönmez Ş, Izquierdo MT, Yücel O (2023) Solution combustion synthesis derived $Li_4SiO_4$ for post-combustion carbon capture. Sep Sci Technol 58(3):573–585. https://doi.org/10.1080/01496395.2022.2136577